Electron Collisions with C_4^- : Detachment Process and Resonant Structure

A. Le Padellec[1], F. Rabilloud[1], D. Pegg[2], K. Andersson[3], D. Hanstorp[3], A. Neau[4], M. Larsson[4], F. Hellberg[4], and R. Thomas[4]

[1]LCAR UMR 5589, Université Paul Sabatier-Toulouse III, 118 route de Narbonne, Bât. III R1B4, 31062 Toulouse Cedex 4, France; [2]Department of Physics, University of Tennessee, Knoxville, Tennessee 37996, USA; [3]Department of Physics, Chalmers University of Technology/Göteborg University, SE- 412 96 Göteborg, Sweden; [4]Department of Physics, Stockholm University, Box 6730, S-113 85 Stockholm, Sweden
arnaud.lepadellec@irsamc.ups-tlse.fr; Franck.rabilloud@lasim.univ-lyon1.fr

1.   INTRODUCTION

A detailed knowledge of the carbon chain's spectroscopy is of considerable importance in astrophysics. More than two decades ago, Douglas[1] put forward the suggestion that the unknown absorbing species responsible for over 150 diffuse interstellar bands, might be long carbon chain molecules, C_n. More recently, Tulej et al.[2] measured the gas phase electronic spectrum of the C_7^- chain and found that the 5 narrow absorption bands in the lowest energy transition correlate quite well with the observed wavelengths of narrow diffuse interstellar bands. CRYRING was used to study collision processes between an electron and a negative ion cluster C_4^-. We made use of a grid to separate four neutral channels over the five that contribute to the total neutral 4C production. Only the detachment cross sections, leading to the production of C_4, are presented here. Although the doubly charged negative ion C_4^{-2} has received little previous attention, a resonance observed in the present work in the threshold region of the detachment cross section is associated with a short lived C_4^{-2} state.

2.   THEORETICAL RESULTS

2.1   Computational Methods

We present a study of the structure of the C_4^- and C_4^{-2} ions. All calculations are carried out using the GAUSSIAN 98 package[3] and are performed in two steps. The geometries of the negative ions are first optimized using the coupled cluster (CC) method involving double substitutions (CCD) in the Hartree-Fock determinant.[4] Restricted Hartree-Fock (RHF) reference wave functions are used for singlet states, and unrestricted Hartree-Fock (UHF) functions for states with higher multiplicities. Various electronic states are considered and several geometrical structures (a $D_{\infty h}$ linear structure, a D_{2h} rhomboid and a C_{2v} three-membered ring) are tested and optimized using a gradient algorithm. In the case of the CCD determined geometries, additional coupled cluster calculations are performed to obtain the total energy of the systems. The CC method involves single and double substitutions, and non-iterative triple excitations (CCSD(T)).[5] In order to reduce the computation time, carbon atoms are represented by relativistic effective pseudo-potentials. In the latter treatment, the 1s electrons are included in the core but only the 2s and 2p electrons are active. Calculations were performed using the linear combination of atomic orbitals (LCAO) scheme. The Gaussian basis set was 5s6p1d. With this basis, the electron affinity of the carbon atom is found to be 0.92 eV. The electron affinity of the C_2 dimer is found to be 2.81 eV, in good agreement with the previous theoretical studies.[6]

2.2   The C_4^- Ion.

The optimized geometries and relative energies of the C_4^- anion are displayed in Fig. 1. The lowest energy isomer A has a linear structure and a $^2\Pi_g$ electronic state. We calculate the length of the central bond to be 1.343 Å, while those of the terminal bonds are 1.277 Å each. These bond lengths compare well with prior calculations.[7-9] Moreover, three other isomers are identified. Isomer B is a $^2\Sigma_g$ linear structure and lies 1.082 eV above isomer A. Isomer C is a planar three membered ring of C_{2v} symmetry and isomer D has a D_{2h} rhombus shape. We find these two latter structures at 1.211 eV and 1.241 eV above A, respectively. For each isomer, we examine the localization of the negative charge using a Mulliken population analysis. The negative charge is localized and shared by the two terminal atoms in isomers A and B. The excess charge is mostly on the terminal carbon atom of the isomer C "tail." For isomer D, the additional negative charge is localized on the two atoms situated on opposite sides of the long diagonal of the rhombus.
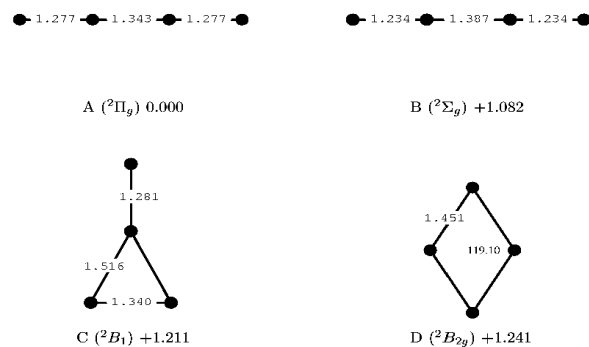
Figure 1. Calculated isomeric structures of the C_4^- ion. Shown are the electronic states, the relative energies (eV) and the atomic separations (Å).

2.3   The C_4^{-2} ion.

The quantum chemistry calculations are extended to C_4^{-2}. In particular, we focus upon the stability of the C_4^{-2} ion with respect to the linear, rhomboidal or three-membered ring isomeric structures. The geometry of the isomers, relative to a minimum in the energy surface, are displayed in Fig. 2. The ground state has a linear structure and a $^1\Pi_g^+$ electronic state. The bond lengths (1.411 Å for the central one and 1.256 Å for the two outer bonds), are close in value to those obtained by a prior ROHF study.[10] The effect on the geometry of C_4^{-2} that results from adding one electron to the C_4^- ion, is an increase in the difference between the central bond and the outer bonds (from 0.066 Å to 0.155 Å). This result, obtained here with correlated calculations, confirms the results from the previous ROHF study,[10] in which the authors suggest a representation of the doubly charged ion as ⁻C   C-C   C⁻. Moreover, the population analysis is in agreement with the intuitive picture since it indicates that the negative charges are mostly localized on the two terminal atoms. A Mulliken analysis indicates -0.8e on each one. A second isomer is found at 1.947 eV above the first one. It has a three-membered ring structure, and a $^1A_1$ ground state. According to a Mulliken analysis, the charge on the terminal carbon of the "tail" is close to -2e. For the rhombus shape, it is found that a ^1A_g state could perhaps be stable, but the single determinant wave function that is used here is not a satisfactory zero order description. Therefore, we do not report it in the present work since it is not expected to be one of the low energy isomers. For completeness, we mention that a few triplet states are considered but no local minima are found in the energy surfaces.
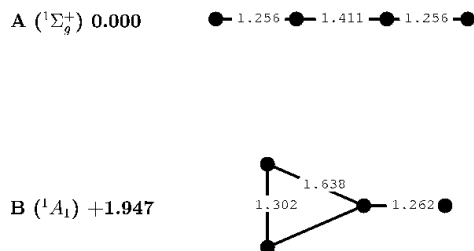
A ($^1\Sigma_g^+$) **0.000**

B ($^1A_1$) **+1.947**

Figure 2. Calculated structures of C_4^{-2}. Shown are the electronic ground state, the relative energy (eV) and the atomic separations (Å).

3.   EXPERIMENTAL RESULTS

The experiment was performed at the heavy ion storage ring, CRYRING, located at the Manne Siegbahn Institute, University of Stockholm, Sweden. C_4^- anions are produced in a sputter ion source.[11] The isomeric composition of the negative ion beam is indeed an important issue in this experiment. Zajfman et al.[12] investigated the photodetachment of negative carbon clusters C_n^-, using a similar sputter ion source. They observed the detachment threshold at about 2.1 eV, which agrees very well with the predicted electron affinity of the rhombus isomer 2.192 eV, rather than with that of 3.75 eV, which would have been expected for a target beam comprised exclusively of the ground state isomer A. On the other hand, Bhardwaj et al.[13] also produced C_4^- projectiles with a sputter ion source but they claim that their ions were predominantly in the A configuration. This is rather puzzling and contradictory evidence.

The following fact led us to adopt Zaijman's findings. Indeed, in the work by Bhardwaj et al., the main goal was not to study the internal excitation of the C_4^- ions as was the case in the Zajfman reference but rather to study collisional dissociation patterns. Moreover, photodetachment experiments (with subsequent threshold characterizations) constitute the sharpest and most reliable test for the evaluation of the internal excitation of a given target. Unfortunately, the drawback is that photodetachment studies do not allow evaluation of the relative proportions of the isomers leaving a given ion source. Therefore, we conclude that the proportions in the various C_4^- isomers remain unknown in the present experiment. Moreover, the relaxation of the C and D isomers to the A configuration prior to any kind of measurement is inefficient, since these isomers are "trapped" in local minima.

We do not present here the operational details of the ring and the analysis procedure since they are included in a companion paper in this book. We give here a few essential numbers concerning the C_4^- target ion beam and the

electron projectiles: the ion beam current after acceleration was typically 770 nA; the ion revolution frequency, often called the Schottky frequency, was 54.42 kHz; the electron beam current and electron density at the 24.77 eV cooling energy, were 0.305 mA and 3.4×10^5 cm^{-3}, respectively.

A detailed description of the reduction of the branching fractions is also included in the companion paper and is not reproduced here. We shall only discuss a few points that are specific to the present study. *Only neutral fragments* resulting from the C_4^- electron interaction were detected in our experiment. The number of counts from the energy sensitive surface barrier detector is plotted against the energy of the given neutral fragment, in a so-called MCA spectrum. The energy of each fragment is a known fraction of the ion beam energy. Thus the four peaks in the MCA spectrum correspond, in increasing order, to C, 2C, 3C and 4C "neutral events". For the electron energy range studied here, 5.0-32.9 eV, the following channels are taken into consideration:

- $\quad C_3^- + C + e - 6.4eV , C_2^- + C^- + C - 10.9eV ,$
  $C_3^+ + C + 3e - 19.7eV , C_2^- + C + C^+ + 2e - 23.0eV ,$
  $C_2^+ + C + C^- + 2e - 25.5eV$
- $\quad C_2^- + C_2 + e - 6.2eV , C_2^- + 2C + e - 12.1eV , C_2 + 2C^- - 12.9eV ,$
  $2C + 2C^- - 18.8eV , C_2 + C_2^+ + 3e - 20.9eV ,$
  $C_2 + C^+ + C^- + 2e - 25.0eV , C_2^+ + 2C + 3e - 26.8eV$
- $\quad C_3 + C^- + e - 7.2eV , C_2 + C + C^- + e - 14.1eV ,$
  $C_3 + C^+ + 3e - 19.3eV , 3C + C^- + e - 20.0eV ,$
  $C_2 + C + C^+ + 3e - 26.2eV$
- $\quad C_4 + 2e - 3.9eV , C_3 + C + 2e - 8.4eV , 2C_2 + 2e - 9.5eV ,$
  $C_2 + 2C2e - 15.4eV , 4C + 2e - 21.3eV ,$

where the four groups of channels contained in the four peaks correspond to the C, 2C, 3C and 4C "neutral events", respectively. The reaction energies are calculated assuming all particles are in their lowest states. Moreover, the estimates do not include contributions from the Coulomb repulsion between the interacting partners in the entrance channel. Fragments associated with several of the above channels appeared in the same peak in the MCA spectrum, and are therefore not distinguishable from each other. In order to determine their relative contributions, i.e. the branching fractions, a grid is inserted in front of the detector. In the present case, the major difference in the analysis of branching fractions compared to the analysis routinely used in dissociative recombination measurements concerns the "redistributed" signal. Here, it does not originate exclusively from the full energy peak 4C, but also from the 3C and 2C peaks. The analysis is, therefore, more complicated and in practice the problem is not fully solvable. Without the grid, we find that the total cross sections for the channels containing at least one charged

carbon fragment, are at least thirty times lower than those for the sum of the five channels for which only neutral carbon atoms (molecules) are produced. We therefore make the simplifying assumption that when the grid is inserted, the C, 2C and 3C peaks grow only at the exclusive expense of the 4C peak.

The cross section curve for the pure detachment channel (C_4 + 2e) is displayed in Fig. 3. The CM energy resolution is about 80 meV at the 6 eV threshold. The error bars on the data points represent only the statistical uncertainties on the cross section measurements, but do not include a 16% systematic uncertainty. Also in Fig. 3, an inset displays the near threshold cross sections. The dashed-dotted line shows a fit to the data using a model cross section, $\sigma=\sigma_0(1-E_{th}^{exp}/E)$, with $E_{th}^{exp}=6.0eV$. The dotted line represents the fit of a Lorentzian function, $s=s_0/\left[(E-E_r)^2+(\Gamma/2)^2\right]$, to the measured data after the dashed-dotted line has been subtracted from it. For this structure, the fit parameters are found to be $E_r=6.75eV$ and $\Gamma=0.93eV$. We believe that this residual structure in the neutral C_4 channel is attributed to a resonance associated with the short-lived doubly charged negative ion, C_4^{-2}. This point is developed below. At 15 eV, the following "channels" are open : C_4 (pure detachment), C_3+C, $2C_2$, C_2+2C, C_3 (Total) and C_2 (Total). They represent 87.1, 2.4, 1.0, 2.6, 4.7 and 2.2 % of the overall flux, respectively. The global dissociation events account for 12.9 % compared with 87.1% for detachment only. Therefore, it appears that one electron is easily detached from the target ion and in most cases, this may be the least tightly bound electron. The detachment only channel dominates overwhelmingly over the numerous fragmentation processes.

The threshold occurs at about 6.0 eV. Part of this value arises from the Coulomb repulsion. We stated that our ion beam was an unknown mixture of the three lowest energy isomers of C_4^-, labeled A, C and D. In that situation, the threshold must be associated with the isomer with the lowest binding energy, the rhombic structure D. Its electron binding energy is 2.2 eV and therefore the pure Coulomb contribution is 3.8 eV (= 6.0-2.2eV). The cross section reaches a maximum value of roughly 2×10^{-16} cm^2. This can be explained from a purely geometrical model. Indeed, one obtains a cross sectional area for the target electron in the ground state linear isomer of 3.3×10^{-16} cm^2. This value might be considered as an upper limit since it is known that other, more compact isomers, such as C and D, populate our ion beam.

The resonance in the threshold region of the pure detachment cross section of Fig. 3 is attributed to a doubly charged negative ion, C_4^{-2}. However, it is difficult to know the isomeric structure of this ion. Nevertheless, we carried out a theoretical search for possible "stable" isomeric structures (see above). The measured width yields a lifetime of 0.7 fs and this value compares very well with the 0.3 fs lifetime that was evaluated[14-15] for C_2^{-2}. The two extra electrons are even closer in this latter

case and therefore the repulsion should be stronger. Therefore, it makes sense that the C_2^{-2} lifetime should be shorter that that for C_4^{-2} . We shall consider the stability of the C_4^{-2} ion with respect to detachment. To do this, one has to
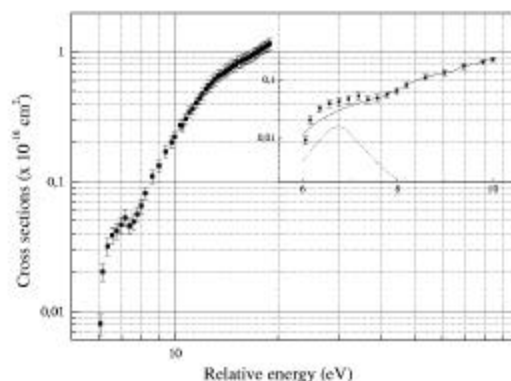

Figure 3. The full squares represent the absolute cross-sections for the pure detachment into C_4 from threshold up to 19 eV. The inset displays the near threshold cross section for pure C_4 detachment. The dashed-dotted line displays a model cross section. The dotted line represents a fit to the data obtained by subtraction of the model cross section fit from the raw experimental data. The fit to this residual structure has the Lorentzian form (see text).

consider the adiabatic electron affinity of the C_4^- ion, which is defined as the energy released when an extra electron is added to C_4^- , the geometry being allowed to relax. The calculations are performed using the CCSD(T) method. For the calculation on the C_4^{-2} dianion, we checked that the *extra electron did not localized on the more diffuse basis functions* and so the electron was really bound to the ion. The electron affinity of the linear C_4^- ion is found to be negative (-2.16 eV), so that the doubly charged negative ion is metastable with respect to the system consisting of the anion plus an infinitely separated electron. In the same way, we find that the adiabatic electron affinity of the three-membered ring C_4^- ($^2B_1$) to the three-membered ring C_4^{-2} is -2.90 eV. Being metastable (short lived) with respect to single detachment, it is reasonable for the C_4^{-2} resonance to decay via single detachment, but we do not have any experimental evidence for this. On the other hand, we do observe that the decay of the dianionic state occurs via double detachment. This indicates that the relaxation might involve more rearrangement within the cluster. Indeed, there might also be the dissociation pathways observed by Mathur et al.[16] Our experimental arrangement do not allow us, however, to intercept the negative fragments necessary to study the production, in coincidence, of $C_2^- + C_2^-$ or/and $C_3^- + C^-$. Mathur et al. carried out a

systematic search for doubly charged negative ions of small carbon clusters formed by laser ablation of graphite. A multicoincidence time-of-flight technique was used to monitor the fragment ion pairs produced by the decay of the doubly charged ions. The two covariance maps that display the formation of these time-correlated $C_2^- + C_2^-$ and $C_3^- + C^-$ ion pairs clearly indicate that C_4^{-2} breaks up preferentially into $C_2^- + C_2^-$. This observation supports our finding concerning the bond lengths in the linear dianion. We found 1.411 Å for the central one and 1.256 Å for the outer two. This, together with the results from the ROHF study,[10] that suggests a representation of the dianion as $^-$C C-C C$^-$, explains why the fragmentation is symmetrical. The central single bond is easier to break than the two outer triple bonds.

4.   CONCLUSION

The results of a study of electron impact detachment of C_4^- are presented. A theoretical approach is used to calculate the geometries of C_4^- and C_4^{-2}. Three different isomers with linear, "three-membered ring" and rhombus structures are associated with the target ion beam but it is not possible to determine their relative populations. Absolute cross sections for pure detachment are presented, with a maximum cross section of 2×10^{-16} cm^2. The corresponding threshold location is found to be approximately 6.0 eV. A resonance with a width of 0.93 eV (0.7 fs lifetime) is observed in the near threshold region. It is attributed to a short lived state of C_4^{-2}. Decay mechanisms for this state are discussed.

ACKNOWLEDGEMENTS

REFERENCES

1   A. E. Douglas, Nature **269**, 130 (1977).
2   M. Tulej, D.A. Kirkwood, M. Pachkov and J.P. Maier, Ap. J, **506**, L69 (1998).
3   M. J. Frisch *et al*, Gaussian 98, Revision A.6 (Gaussian Inc., Pittsburgh, 1998).
4   J. A. Pople, R. Krishnan, H. B. Schlegel and J. S. Binkley, Int. J. Quant. Chem. **14,** 545 (1978).
5   K. Raghavachari, G. W. Trucks, J. A. Pople and M. Head-Gorden, Chem. Phys. Lett. **157**, 479 (1989).
6   J. D. Watts and R. J. Bartlett, J. Chem. Phys. **96**, 6073 (1992).

7   J. D. Watts, J. Gauss, J. F. Stanton and R. J. Bartlett, J. Chem. Phys. **97**, 8372 (1992).

8   A. K. Ray and B. K. Rao, Z. Phys. D. **33**, 197 (1995).

9   S. Schmatz and P. Botschwina, Int. J. Mass Spectrom. Ion Proc, **149/150**, 621 (1995).

10   J. D. Watts and R. J. Bartlett, J. Chem. Phys. **97**, 3445 (1992).

11   Peabody Scientific, Peabody, Massachusetts, USA

12   Z. Vager, H. Feldman, D. Kella, E. Malkin, E. Miklazky, D. Zajfman and R. Naaman, Z. Phys. D - At. Mol. Cl. **19**, 413 (1991).

13   V. R. Bhardwaj, C.P. Safvan, D. Mathur, and A.K. Gupta, Int. J. Mass Spec. Ion. Phys.**163**, 141 (1997).

14   H.B. Pedersen, N. Djuric, M.J. Jensen, D. Kella, C.P. Safvan, L. Vejby-Christensen and L. H. Andersen, Phys. Rev. Lett. **81,** 5302 (1998).

15   L. H. Andersen, P. Hvelplund, D. Kella, P. H. Mokler, H. B. Pedersen, H. T. Schmidt and L. Vejby-Christensen, J. Phys. B **29,** L643 (1996).

16   D. Mathur, V. R. Bhardwaj, F. A. Rajgara and C. P. Safvan, Chem. Phys. Lett. **277,** 558 (1997).